AIChE

PROCESS SYSTEMS ENGINEERING

Fault Detection and Isolation in Hybrid Process Systems Using a Combined Data-Driven and Observer-Design Methodology

Chudong Tong
Key Laboratory of Advanced Control and Optimization for Chemical Processes of Ministry of Education, East China University of Science and Technology, Shanghai 200237, P.R. China

Dept. of Chemical Engineering and Materials Science, University of California, Davis, CA 95616

Nael H. El-Farra and Ahmet Palazoglu
Dept. of Chemical Engineering and Materials Science, University of California, Davis, CA 95616

Xuefeng Yan
Key Laboratory of Advanced Control and Optimization for Chemical Processes of Ministry of Education, East China University of Science and Technology, Shanghai 200237, P.R. China

DOI 10.1002/aic.14475
Published online April 30, 2014 in Wiley Online Library (wileyonlinelibrary.com)

A combined data-driven and observer-design methodology for fault detection and isolation (FDI) in hybrid process systems with switching operating modes is proposed. The main contribution is to construct a unified framework for FDI by integrating Gaussian mixture models (GMM), subspace model identification (SMI), and results from unknown input observer (UIO) theory. Initially, a GMM is built to identify and describe the multimodality of hybrid systems using the recorded input/output process data. A state-space model is then obtained for each specific operating mode based on SMI if the system matrices are unknown. An UIO is designed to estimate the system states robustly, based on which the fault detection is laid out through a multivariate analysis of the residuals. Finally, by designing a set of unknown input matrices for specific fault scenarios, fault isolation is performed through the disturbance-decoupling principle from the UIO theory. A significant benefit of the developed framework is to overcome some of the limitations associated with individual model-based and data-based approaches in dealing with the problem of FDI in hybrid systems. Finally, the validity and effectiveness of the proposed monitoring framework are demonstrated using a numerical example, a simulated continuous stirred tank heater process, and the Tennessee Eastman benchmark process. © 2014 American Institute of Chemical Engineers *AIChE J*, 60: 2805–2814, 2014
Keywords: fault detection and isolation, hybrid process systems, unknown input observer, data-driven techniques

Introduction

The effective and timely monitoring of chemical processes is of paramount importance in process systems engineering to ensure safety and to achieve high-quality, consistent products. Not surprisingly, the increasing demands for more rigorous monitoring in chemical processes continue to draw attention in both the academic and industrial circles.[1–4] Significant progress has been achieved over the past few decades by introducing approaches that use causal models for model-based fault detection and isolation (FDI), as well as multivariate statistical process control (MSPC), referred to as data-driven techniques. Compared to MSPC, model-based methods are based on the concept of analytical or functional redundancy, which make use of a mathematical model of the process to accurately describe complex dynamic behavior and tend to give more accurate results.[5] However, as the complexity of modern industrial processes increases, the development of such a model becomes difficult, sometimes, even impossible.[6] As a class of alternatives, the data-driven techniques present a potential solution to model construction and fault detection for large-scale processes and find wide applications in various industrial processes resulting from its conceptual simplicity and practical usefulness.[6,7] Although MSPC has no requirement of prior system knowledge, the general lack of an accurate description of the dynamic process behavior may yield ambiguous and misleading results.[8]

An examination of the existing literature for model-based FDI shows that the observer-design has become the most popular and established method, especially within the automatic control community.[9,10] A theoretical framework of unknown input observers (UIO) for robust FDI has been developed in the past years.[10–12] The UIO theory, which is based on the disturbance decoupling principle, has been used

Correspondence concerning this article should be addressed to N. H. El-Farra at nhelfarra@ucdavis.edu.

© 2014 American Institute of Chemical Engineers

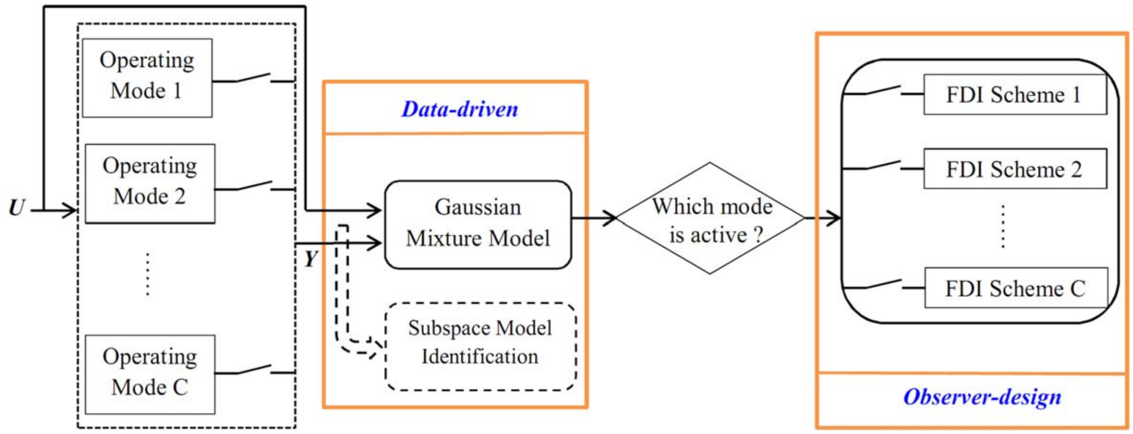

Figure 1. Overview of the hybrid monitoring framework.

[Color figure can be viewed in the online issue, which is available at wileyonlinelibrary.com.]

for sensor fault isolation and actuator failure detection.[3] Related to UIO, input estimation or reconstruction of system inputs have also been proposed for the detection of sensor and actuator faults.[13,14] However, the difficulties in obtaining a causal model are not adequately discussed in the literature and applications are typically limited to numerical examples or small-scale systems.[15] In contrast, data-driven techniques can handle large-scale processes since only historical process data is required.[16–19] This category of approaches has gained considerable attention in recent years. Furthermore, significant progress has been made in the data-mining and processing area, which can provide new technologies for the utilization of FDI. The main disadvantage of MSPC is that it may not function well if the process exhibits a significant dynamic behavior.[8] To overcome the limitations of individual approaches, several studies have been performed for the combination of model-based FDI and MSPC. Sotomayor and Odload[10] and Ding et al.[20] examined the incorporation of subspace model identification (SMI) into model-based FDI to handle the modeling task for large-scale systems. Schubert et al. proposed a unified scheme that integrates model-based and multivariate statistical methods recently.[15,21] Other examples of approaches that combine model-based and data-based techniques for FDI include the results in Ohran et al.[22,23]

Despite a rich body of literature on process monitoring, the majority of existing methods have been developed for purely continuous processes with only a single operating condition. However, many chemical processes are operated under substantially different operating regimes and are more appropriately modeled as hybrid systems. As a result, the multimodality of a hybrid system is characterized by switching between a finite number of operating modes or subsystems. Research on hybrid process monitoring has mainly focused on developing monitoring schemes using either model-based or data-driven approaches.[24–26] Generally, the most important task in the design of FDI schemes for hybrid systems with switching modes is the identification and description of the constituent operating modes. An effort to address these issues was initiated in Hu and El-Farra,[24] where a family of mode observers was designed in a way that facilitates the identification of the active mode without information from controllers. However, the design of the mode observers requires certain constraints on the system structure to ensure decoupling the influence of disturbances and local faults on the mode transition residuals. The approach also requires sufficiently accurate information about the state-space models of the constituent subsystems. To relax these limitations and enlarge the class of hybrid process systems that can be considered, an alternative mode identification scheme needs to be developed and incorporated into the hybrid system monitoring structure. Another key issue that needs to be addressed is the ability of the fault isolation scheme to diagnose abnormal situations effectively. Although MSPC has no requirement for prior system knowledge, conventional fault diagnosis using contribution plots, variable reconstruction, or statistical discriminate analysis may yield ambiguous and misleading results given that the underlying process dynamics is insufficiently or inaccurately described. To avoid this, a fault isolation scheme that can accurately distinguish between different faults needs to be developed.

To tackle these challenges, we develop in this work a framework for FDI of hybrid processes with switching modes. This framework brings together ideas and concepts from the data-driven and observer-design methodologies by integrating Gaussian mixture models (GMM), SMI, and techniques from UIO theory. Initially, a GMM is built to identify and describe the multimodality of hybrid systems using the recorded input/output process data. Then, a state-space model for each specific operating mode is obtained based on SMI. Next, an UIO is designed to estimate the system states robustly, and a multivariate analysis of the residuals is conducted to detect the faults. Finally, a set of unknown input matrices are designed for specific fault scenarios, and fault isolation is performed through the disturbance-decoupling principle from UIO theory. A key advantage of combining data-driven and observer-design methodologies for hybrid process monitoring is the ability to overcome the limitations of individual approaches and to enlarge the class of hybrid process systems for which the FDI problem can be addressed.

Overview of Hybrid Process Monitoring Framework

An overview of the proposed monitoring framework is schematically depicted in Figure 1. For multimodal processes, it is reasonable to assume that the process data of each individual mode possesses a specific data characteristic. Based on this, GMM can be used for mode identification and description. For this purpose, only historical data are required, and the structural constraints of the mode observers considered in Hu and El-Farra[24] can be relaxed. Furthermore, practical experience has shown that many industrial processes can be approximated with sufficient accuracy by linear time-invariant systems of finite dimensions. Thus, the identified state-space models that describe the dynamics of normal conditions are faithful representations for each operating mode if the accurate first-principle model is difficult to obtain.

Once the active mode is identified, detection and isolation of faults within the active mode needs to be performed. To this end, the UIO is adopted here for the purpose of residual generation, and then a multivariate statistic, T^2, is calculated as the fault indicator, which takes the residual correlation into consideration. The fault alarm is triggered once the T^2 statistic violates its corresponding control limit obtained from an F-distribution.[1] Fault isolation is an issue that is not adequately investigated for hybrid process systems. Motivated by the decoupling-principle from UIO theory, a set of unknown input matrices can be designed to compensate for specific fault scenarios. Given that the isolated fault is decoupled from residual generation, only the UIO with the corresponding unknown input matrix would generate a T^2 statistic that shows insignificant variation.

The following sections provide a detailed description of the design and implementation of the proposed framework for FDI of hybrid processes with switching modes.

Data-Driven Mode Identification and SMI

This section presents a brief summary of GMM and SMI that will be used for mode identification and state-space model development.

Gaussian mixture model

The assumption of multivariate Gaussian distribution becomes invalid owning to the multiple operating modes featured by mean shifts and/or covariance changes. In this situation, however, the multiple operating modes can still be characterized by a mixture of local Gaussian components. Therefore, the finite GMM is well suited for describing the different modes. Suppose $\boldsymbol{s}$ is a sample vector from a historical multimodal process dataset. The GMM is a probabilistic model represented by a weighted average of Gaussian probability density functions describing a set of production modes[27]

$$p(\boldsymbol{s}|\boldsymbol{\theta})=\sum_{i=1}^{C} w_i N(\boldsymbol{s}|\boldsymbol{\mu}_i, \boldsymbol{\Sigma}_i) \tag{1}$$

where C is the number of Gaussian components, which should be equal to the number of all possible normal operating modes. $\boldsymbol{\theta}$ is a parameter vector whose entries are model parameters (i.e., cluster probability w_i, mean vector $\boldsymbol{\mu}_i$, and covariance matrix $\boldsymbol{\Sigma}_i$ of the i-th component). $N(\boldsymbol{s}|\boldsymbol{\mu}_i, \boldsymbol{\Sigma}_i)$ denotes the multivariate Gaussian density function for the i-th component. The parameters can be obtained by an expectation-maximization (EM) algorithm. A major limitation of the basic EM algorithm, however, remains that the number of Gaussian components has to be prespecified and cannot be adjusted automatically. To overcome this drawback, the F-J algorithm[28] is adopted here to automatically determine the number of Gaussian components (or operating modes), C.

When the GMM is used as part of an online mode identification procedure, the posterior probability of the currently sampled data $\boldsymbol{s}_{\text{new}}$ belonging to each Gaussian component can be used as the mode indicator, given as follows

$$p(\boldsymbol{s}_{\text{new}} \in c)=\frac{w_c N(\boldsymbol{s}_{\text{new}}|\boldsymbol{\mu}_c, \boldsymbol{\Sigma}_c)}{\sum_{i=1}^{C} w_i N(\boldsymbol{s}_{\text{new}}|\boldsymbol{\mu}_i, \boldsymbol{\Sigma}_i)} \tag{2}$$

where the denominator serves as a scaling factor such that the sum of posterior probabilities is 1. Abbreviating the operating mode by op, the target $\text{op}=\arg\max\{p(\boldsymbol{s}_{\text{new}} \in c), c=1,2,\ldots,C\}$ is the corresponding identified operating mode for the measurement $\boldsymbol{s}_{\text{new}}$.

Remark 1. *It is important to note that the use of the EM algorithm for the identification of the GMM is not necessary. This is important given the well-known numerical and computational costs associated with the EM algorithm which could limit its applicability in situations involving large-scale industrial processes. An alternative—and less computationally burdensome—approach that can be used instead is the one proposed by Feital et al.[26] This approach consists of a two-step clustering approach that is used to estimate the GMM and avoid the drawbacks of the EM algorithm. Dimensionality reduction is conducted in the first step, and then the GMM parameters are obtained without significant effort. The same idea can be adopted within the monitoring framework proposed in this work when the GMM is applied to characterize a large-scale multimodal process. Indeed, a review of existing work on dimensionality reduction shows that there are many unsupervised dimensionality reduction algorithms that can be used without destroying the cluster structure.[29–31] These methods can also be used as a preprocessor if the GMM identification scheme encounters computational issues.*

Subspace model identification

Approaches for model-based FDI typically require the construction of a first-principle model of the process, which is usually not feasible for complex industrial systems. As an alternative to first-principle models, subspace identification methods allow an estimation of the state-space model using recorded input/output process data.[17,32] Furthermore, practical experience has shown that many industrial processes can be approximated with sufficient accuracy by linear time-invariant systems of finite dimensions. Motivated by this, we consider in this work hybrid process systems with switching modes that can be approximated by the following state-space representation

$$\begin{aligned} \boldsymbol{x}(k+1)&=\boldsymbol{A}_i\boldsymbol{x}(k)+\boldsymbol{B}_i\boldsymbol{u}(k)+\boldsymbol{w}_i(k) \\ \boldsymbol{y}(k)&=\boldsymbol{C}_i\boldsymbol{x}(k)+\boldsymbol{D}_i\boldsymbol{u}(k)+\boldsymbol{v}_i(k) \end{aligned} \tag{3}$$

where $i \in \{1,2,\ldots,C\}$ denotes the corresponding operating mode, $\boldsymbol{x}(k) \in R^n$ is the state vector, $\boldsymbol{y}(k) \in R^l$ is the output vector, $\boldsymbol{u}(k) \in R^m$ is the input vector, $\boldsymbol{w}_i(k) \in R^n$, and $\boldsymbol{v}_i(k) \in R^l$ are the process noise and measurement noise, respectively. In some cases, it is possible to express the vector $\boldsymbol{w}_i(k)$ as: $\boldsymbol{w}_i(k)=\boldsymbol{E}_i\boldsymbol{d}(k)$, where $\boldsymbol{E}_i$ is the unknown input distribution matrix.

It should be noted that since the identified SMI model is accompanied by model uncertainties and dynamics, the accuracy of the identified model becomes a crucial factor for any model-based method. In recent years, SMI methods have enjoyed rapid development for both closed-loop and open-loop processes.[32] Different approaches have been proposed and detailed description can be found in the literature. In this article, the free subspace identification toolbox developed by Overschee[33] is adopted, and the identified state-space model is expected to provide a good approximation of the causal relationship between the input and output variables.

Observer-Design for FDI in Hybrid Systems

Fault detection based on UIO

The most important task in model-based FDI is the generation of residuals. To increase the robustness of the state estimation, the literature advocates the use of UIOs to decouple the state estimation error from the unknown inputs or disturbances. Following Simani et al.,[3] we design a UIO for each specific mode with the following form

$$\begin{aligned} z(k+1) &= F_i z(k) + T_i B_i u(k) + K_i y(k) \\ \hat{x}(k) &= z(k) + H_i y(k) \end{aligned} \tag{4}$$

with $z(k) \in R^n$ is the state vector of the UIO, $\hat{x}(k)$ is the estimate of the state vector $x(k)$, while F_i, T_i, K_i, H_i are matrices that will be designed for mode $i \in \{1, 2, \cdots, C\}$ such that the unknown input will be decoupled from other inputs. The design of a UIO as well as the necessary and sufficient existence conditions are presented in Simani et al.[3] It is worth noting that without the unknown inputs matrix E_i in the system, the observer reduces to the standard Luenberger observer.

The presence of a fault can be described by examining the mismatch between Eq. 3 and the state estimate $\hat{x}(k)$

$$\begin{aligned} \Delta\hat{x}(k+1) &= \hat{x}(k+1) - \hat{x}(k+1|k) \\ &= \hat{x}(k+1) - (A\hat{x}(k) + Bu(k)) \end{aligned} \tag{5}$$

where $\hat{x}(k+1|k)$ is the model prediction of the state vector for sample $k+1$ using the state estimate $\hat{x}(k)$, and the control input $u(k)$ from the previous step. Given that the identified state-space first describes the input to state relationship and then the state to output relationship, the generated state residual $\Delta\hat{x}(k+1)$ is sensitive to sensor, actuator and process faults. According to Eq. 5, $\Delta\hat{x}(k+1)$ is assumed to follow a zero-mean multivariate Gaussian distribution under normal operating conditions. Therefore, any significant change in the Hotelling's T^2 statistic as defined in Eq. 6 below is indicative of the presence of a fault

$$T^2 = \Delta\hat{x}(k+1)^T S_{\Delta\hat{x}}^{-1} \Delta\hat{x}(k+1) \tag{6}$$

where $S_{\Delta\hat{x}}$ is the error covariance matrix of a reference data set. The corresponding control limits can be determined from an F-distribution with degrees of freedom n and $N-n$, where $N$is the number of reference samples in each operating mode. For a given significance level α, the T^2 statistic yields $T^2 \leq T^2_\alpha$ under normal operating conditions, while we have $T^2 > T^2_\alpha$ during abnormal operating conditions.

Remark 2. *While the assumption that the constituent modes exhibit linear dynamics may be reasonable for many industrial processes, it may also impose limitations, especially when dealing with highly nonlinear processes. It should be noted, however, that the focus of the proposed monitoring scheme is mainly on bringing together the model-based and data-driven techniques to address the fault diagnosis problem in hybrid processes that switch between a finite set of subsystems. In this context, the assumption that the dynamics of the constituent subsystems are linear is made primarily to simplify the development and presentation of the key ideas. This assumption can be relaxed, and the same monitoring framework can be extended to deal with nonlinear hybrid systems—where the constituent modes are governed by nonlinear dynamics—using nonlinear model-based FDI techniques developed in the literature[34–36]. Furthermore, the dataset for training the GMM is fault-free; therefore, the assumption of locally Gaussian distribution within each operating mode is reasonable. Different faults present different degrees of nonlinearity in the sampled process data; however, the faulty dataset is not used in the off-line modeling phase, and the change of nonlinearity, mean, covariance, or other attributes for the online sampled data can be detected as faults by the proposed monitoring method.*

Sensor fault isolation

Apart from the measurement noise, the vector $v(k)$ in Eq. 3 can also represent sensor faults. In the presence of sensor faults, robust state estimation is achieved by augmenting the system model with faulty sensor characteristics. More precisely, the faulty sensor measurements can be described by the following system[12,37]

$$v(k+1) = A_v v(k) + \xi(k) \tag{7}$$

with dynamics described by A_v and the unknown additive sensor fault $\xi(k) \in R^r (r \leq l)$. Therefore, the augmented state-space model is given as

$$\underbrace{\begin{bmatrix} x(k+1) \\ v(k+1) \end{bmatrix}}_{x_a(k+1)} = \underbrace{\begin{bmatrix} A_i & \\ & A_v \end{bmatrix}}_{A_a} \underbrace{\begin{bmatrix} x(k) \\ v(k) \end{bmatrix}}_{x_a(k)} + \underbrace{\begin{bmatrix} B_i \\ 0 \end{bmatrix}}_{B_a} u(k) + \underbrace{\begin{bmatrix} 0 \\ I \end{bmatrix}}_{E_a} \xi(k) \tag{8}$$

$$y(k) = [\,C_i \quad I\,] x_a(k) + D_i u(k) \tag{9}$$

Consequently, the state estimation error obtained by UIO is decoupled from the sensor fault. Isolating which sensor is faulty and extracting the magnitude and signature of the sensor fault relies on these augmented UIOs. Assuming that the i-th sensor is faulty, only the augmented UIO that includes the i-th sensor fault as an additional state will generate a T^2 statistic that shows no significant change.

Actuator and process fault diagnosis

In contrast to simple sensor faults, actuator and process faults isolation cannot be performed in a similar way to sensor faults. For FDI applications, input reconstruction or estimation has been proposed for diagnosis of actuator and process faults. This can be addressed by reconstructing the system inputs $u(k)$[15]

$$\hat{u}(k) = B^*(\hat{x}(k+1) - A\hat{x}(k)) \tag{10}$$

where B^* is the generalized inverse of B. This gives rise to the formulation of input residuals

$$\Delta\hat{\boldsymbol{u}}(k)=\boldsymbol{B}^{*}(\hat{\boldsymbol{x}}(k+1)-\boldsymbol{A}\hat{\boldsymbol{x}}(k)-\boldsymbol{B}\boldsymbol{u}(k)) \tag{11}$$

It is worth noting that the interpretation of input residuals is that $\Delta\hat{\boldsymbol{u}}(k)$ can describe the required information for compensating the fault condition.

Remark 3. *For complex industrial processes, the reliable diagnosis of faults can be a challenging task for both model-based and statistical-based methods. Although the above input reconstruction technique can be implemented by an accurate mathematical plant description, it might not be well suited for the identified state-space model given that it only captures the dynamics of normal conditions, and not the underlying mechanism of the system. For some results on model-based actuator fault isolation, the reader is referred to literature.*[34–36] *In general, however, sensor faults are more likely to be encountered in such complex processes and it is essential to have a sensor fault diagnosis method.*

The following section presents case studies to demonstrate the capability of the proposed framework to monitor hybrid process systems with switching modes. It should be emphasized that the proposed approach is designed for hybrid processes that switch "instantaneously" between the constituent dynamic modes, so that there are sharp and unambiguous transitions between the different dynamics. In other words, the time it takes the process to switch from one set of dynamics (e.g., one governing set of differential equations) to another is assumed to be negligible compared with the residence time that the process spends in a given mode (the "dwell time"). Consideration of the transition intervals between the different modes, while possible, may lead to biased mode characterization and identification results, and is thus not attempted in this work. Instead, sharp mode transitions are considered in the following testing cases. This implies that the total operation time is simply the sum of the dwell times of the individual modes, and that the state of the system at any time is governed by only a distinct and identifiable set of dynamics. This eliminates any ambiguity in mode identification. For results on monitoring multimodal processes with transition dynamics, the reader is referred to the literature.[38,39]

While the transition intervals between the modes are not considered, the transients within the constituent modes are taken explicitly into account in the developed monitoring framework. Specifically, within each mode, the process state is allowed to go through a transient phase before it settles at (or close to) the corresponding steady state. We consider scenarios where the process state dwells within each mode long enough to approach the corresponding steady state (i.e., the dwell time is much larger than the settling time). Given the fact that the dwell time is finite, and the fact that in principle a system attains steady state only in infinite time, for practical purposes the settling time can be used as an indicator that the state has converged sufficiently close to the desired equilibrium point.

Illustration and Discussion

Numerical example

In this subsection, a hybrid system with two distinct operating modes is considered first. The hybrid system has the following state-space model

$$\begin{aligned}\boldsymbol{x}(k+1)&=\boldsymbol{A}_i\boldsymbol{x}(k)+\boldsymbol{B}\boldsymbol{u}(k)\\ \boldsymbol{y}(k)&=\boldsymbol{C}\boldsymbol{x}(k)+\boldsymbol{D}\boldsymbol{u}(k)+\boldsymbol{v}(k)\end{aligned} \tag{12}$$

with $\boldsymbol{A}_1=\begin{bmatrix}0.118 & -0.191 & 0.287\\ 0.874 & 0.264 & 0.943\\ -0.333 & 0.514 & -0.217\end{bmatrix}$, $\boldsymbol{A}_2=\begin{bmatrix}0.161 & -0.393 & 0.812\\ 0.467 & 0.368 & 0.968\\ -0.433 & 0.541 & -0.197\end{bmatrix}$, $\boldsymbol{B}=\begin{bmatrix}1 & 2\\ 3 & -4\\ -2 & 1\end{bmatrix}$, $\boldsymbol{C}=\begin{bmatrix}-0.72 & 0.21 & -0.05\\ -0.20 & 0.06 & 0.35\\ -0.66 & -0.22 & -0.01\\ 0.45 & -0.295 & -0.158\end{bmatrix}$, and $\boldsymbol{D}=0$

The system inputs are given by

$$\begin{aligned}\boldsymbol{u}(k+1)=&\begin{bmatrix}0.811 & -0.226\\ 0.477 & 0.415\end{bmatrix}\\ &\times\boldsymbol{u}(k)+\begin{bmatrix}0.193 & 0.689\\ -0.320 & -0.749\end{bmatrix}\cdot\begin{bmatrix}\boldsymbol{w}_1(k)\\ \boldsymbol{w}_2(k)\end{bmatrix}\end{aligned} \tag{13}$$

where $\boldsymbol{v}(k)$ is the measurement noise with zero mean and a standard deviation of 0.2, and $[\boldsymbol{w}_1(k)\boldsymbol{w}_2(k)]^T$ denotes Gaussian distributed data sources. Two different sets of data sources are simulated to represent different operating modes as follows

Mode 1: $\boldsymbol{w}_1(k):N(10,0.8^2);\boldsymbol{w}_2(k):N(12,0.6^2)$
Mode 2: $\boldsymbol{w}_1(k):N(6,0.9^2);\boldsymbol{w}_2(k):N(16,0.7^2)$

where the means and variances of $\boldsymbol{w}_1(k)$ and $\boldsymbol{w}_2(k)$ are changed to reflect the shifts of operating modes. The deviations of the true inputs from the measured nominal inputs $\boldsymbol{u}(k)$ are unknown, this gives rise to set $\boldsymbol{E}=\boldsymbol{B}$ given that the unknown portion superimposes the measured value has the same dynamic characteristic $\boldsymbol{B}$.

In this simulation, the system is assumed to be running under the above defined two conditions with equal probabilities. The data vector for analysis consists of $[\boldsymbol{u}(k);\boldsymbol{y}(k)]$ and 500 samples under each operating mode are generated as the historical database. Then, all the 1000 samples are used as training data to construct a GMM. Given that an accurate model is already known, an UIO is directly designed for each mode and stored for online monitoring. To illustrate the utility of the proposed monitoring strategy, two fault scenarios are considered and listed in Table 1.

When a new sampled data becomes available, the online monitoring entails the following three steps:

1. Identify the current operating mode. Using Eq. 2, the current operating mode op can be identified. The mode identification results for the two cases are given in Figures 2a, b, respectively, where it can be seen that the operating mode is correctly identified even in the presence of various faults and variations in the individual modes.
2. Determine whether the process operates in normal conditions or not. After the current op is identified, the

Table 1. Fault Scenarios for the Numerical Example

No.	Mode	Test Scenario	Period
Case 1	2	Normal operation	1–150
	2	Random variation of sensor y_1	151–300
	2	Normal operation	301–800
	1	Normal operation	801–1000
	1	Step change of sensor y_3	1001–1150
	1	Normal operation	1151–1600
Case 2	1	Normal operation	1–200
	1	Step change of input u_1	201–350
	1	Normal operation	351–1000
	2	Normal operation	1001–1200
	2	Random variation of input u_2	1201–1600

corresponding FDI scheme is activated. The T^2 statistic is constructed to indicate faults. The plots in Figure 3 show that the residuals under abnormal conditions violate the T^2 control limit with a significance level of $\alpha=99\%$.

3. After a fault has been detected, fault isolation is then performed. For sensor fault isolation, a bank of UIOs was designed. Specifically, a UIO was designed for each augmented system with one additional output variable. Given that each augmented system contains one output variable, the matrix $\boldsymbol{A}_v$ matrix in Eq. 7 reduces to a scalar and its value is chosen to be 0.8. Identifying the faulty sensor relies on the use of individual T^2 indices. As shown in Figure 4, only the T^2 for the UIO augmented with sensor y_1 (upper plot) and T^2 for the UIO augmented by sensor y_3 (lower plot) did not present any significant violation. Therefore, the sensor faults for each mode are isolated successfully. As for actuator fault isolation, the input residual in Eq. 11 is used to analyze the root cause for these abnormal events. Figure 5 highlights that input u_1 under Mode 1 and input u_2 under Mode 2 are the isolated faulty units.

To demonstrate the advantages of the proposed method over purely statistically based monitoring methods, the multiple principal component analysis (PCA) approach[25] is introduced here for comparison. Multiple PCA is based on the idea of building a local PCA model for each operating mode, and then having each monitored sample categorized

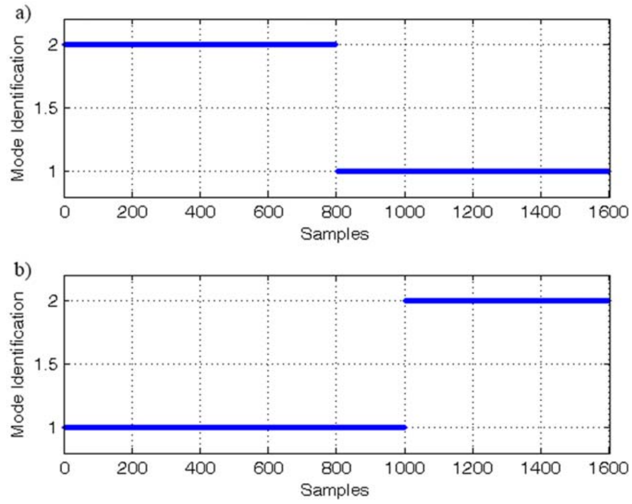

Figure 2. Mode identification results for (a) Case 1 and (b) Case 2.

[Color figure can be viewed in the online issue, which is available at wileyonlinelibrary.com.]

into a specific PCA model. The T^2 statistic for the systematic part of the process variation and the Q statistic for the residual part of the process variation are then used as fault indicators.[25] The monitoring results for the two fault scenarios are reported in Figure 6. It should be noted that the results from different local PCA models are manually put together. It can be seen that the multiple PCA method is unable to detect the sensor and actuator faults consistently and reliably. Given that the PCA-based monitoring method does not require the existence of autocorrelation in the underlying measured process data, it is ill suited for dynamic process monitoring with autocorrelation. This observation points to the major benefit of including the observer-design FDI methodology within the hybrid monitoring scheme.

Simulated CSTH example

In this subsection, the proposed monitoring framework is applied to a simulated CSTH process under multiple operating conditions. The closed-loop simulation of the CSTH pilot-plant was originally developed by and can be found in Thornhill et al.[40] The stirred tank is supplied with well-

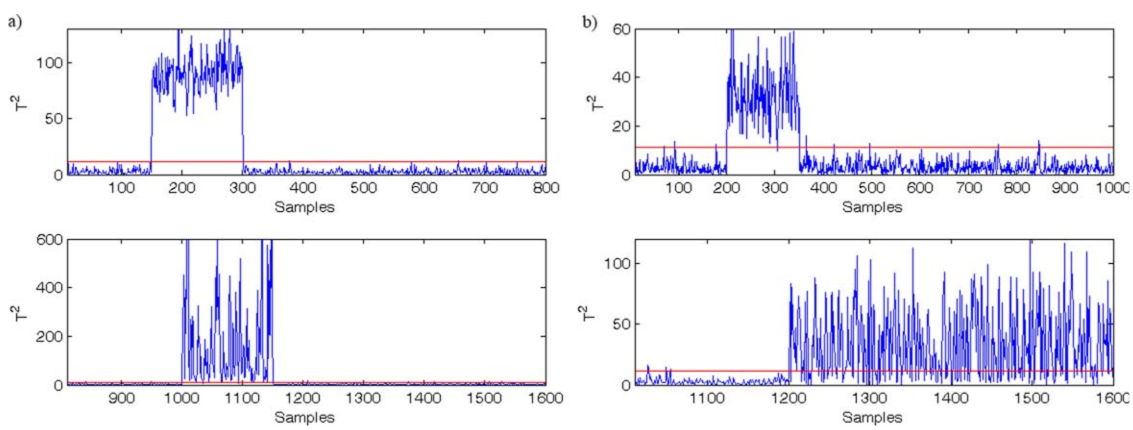

Figure 3. T^2 statistic with 99% control limit (red solid line) for the monitoring of (a) Case 1 changing from Mode 2 (top left) to Mode 1 (bottom left), and (b) Case 2 changing from Mode 1 (top right) to Mode 2 (bottom right).

[Color figure can be viewed in the online issue, which is available at wileyonlinelibrary.com.]

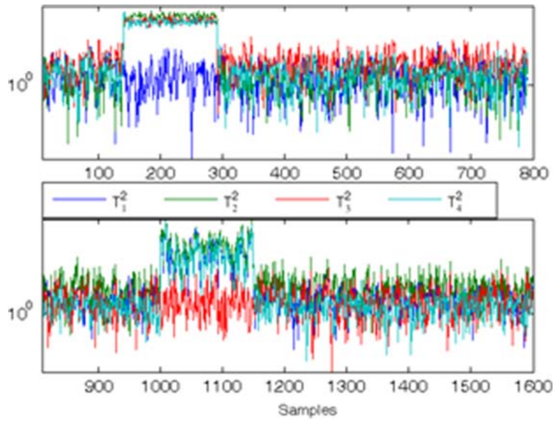

Figure 4. Sensor fault isolation for Case 1 under Mode 2 (top) and Mode 1 (bottom).

[Color figure can be viewed in the online issue, which is available at wileyonlinelibrary.com.]

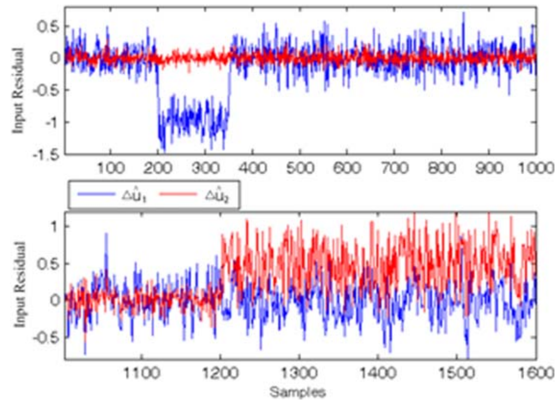

Figure 5. Actuator fault isolation for Case 2 under Mode 1 (top) and Mode 2 (bottom).

[Color figure can be viewed in the online issue, which is available at wileyonlinelibrary.com.]

mixed hot and cold water (HW and CW) as well as steam. The process outputs are the electronic measurements of the level, temperature, and CW flow rate. A full description of the CSTH process can be found in Thornhill et al.[40] and the closed-loop simulation programs are available at their website.[41] As listed in Table 2, three sets of operating conditions on the level set-point, temperature set-point, and HW valve are designed to test the performance of the proposed method in monitoring this kind of hybrid system with multiple modes. Note that, unlike the previous example, mode transitions are triggered by changes in the control system, and not by the autonomous dynamics of each operating mode.

In the training period, 500 samples are generated under each operating mode with 1 s sampling time and all 1500 samples are used for constructing the nominal GMM. It is noted that two inputs (steam valve and CW valve positions) and three outputs (tank level, temperature, and CW flow rate) are selected for this study. By feeding the data into the GMM learning framework, a three-component GMM is obtained. Subsequently, the SMI method is used to generate a linear state-space model for each mode. Afterward, a family of Luenberger state observers is designed based on the identified state-space models. A confidence level of 99% is selected for calculating the control limits for the T^2 statistic.

For illustration purposes, the abnormal scenario given in Table 3 is considered. As depicted in Figure 7, the operating mode is successfully identified. Based on this mode identification result, the T^2 statistic together with the control limit is outlined in Figure 8. It is obvious that the T^2 statistic violates its control limit after a fault occurs.

Once a fault is detected, the diagnosis of that fault becomes the next critical task. In this example, only sensor fault isolation under Mode 2 is implemented through the design of a bank of three different augmented UIOs. With the number of unknown sensor fault $r=1$, the matrix $\boldsymbol{A}_v$ in Eq. 7 reduces to a scalar and is also chosen to be 0.8. Figure 9 shows the individual statistics for the augmented UIOs and confirms that only the augmented UIO for the first sensor y_1 does not produce any significant violation, thus indicating the first sensor is abnormal.

Application to TE benchmark process

The TE benchmark process has been widely used to test the performance of various control and monitoring methods.[20,42–44] As illustrated in Downs and Vogel,[42] there are five major unit operations, which include a chemical reactor, a condenser, a recycle compressor, a stripper, and a vapor/liquid separator. The TE process has six different operating modes available for simulation case studies. Detailed descriptions are well explained in Chiang et al.[16] The original process is strictly open-loop unstable, and the decentralized control strategy proposed by Ricker[44] is adopted for the closed-loop process operation. The MATLAB simulation

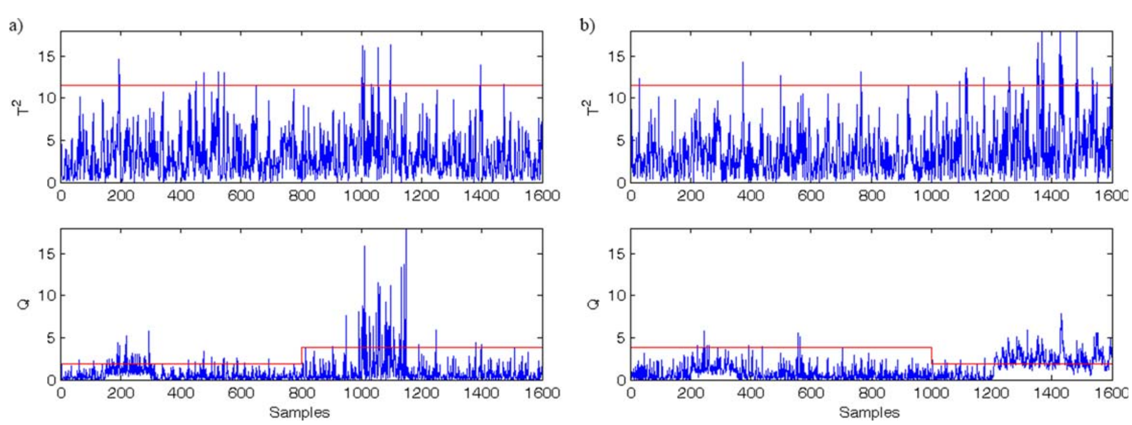

Figure 6. Fault detection results based on multiple PCA for (a) Case 1 and (b) Case 2.

[Color figure can be viewed in the online issue, which is available at wileyonlinelibrary.com.]

Table 2. Normal Operating Modes of the CSTH

Set-Points	Mode 1	Mode 2	Mode 3
Level	12	12	16
Temperature	10.5	8	10.5
HW Valve	5.5	4	5

Table 3. Test Scenario of the Simulated CSTH

Mode No.	Test Scenario	Period
3	Normal operation	1–160
3	Hot water temperature step change (process fault)	161–400
3	Normal operation	401–600
1	Normal operation	601–800
1	Tank level sensor fault (y_1)	801–1000
1	Normal operation	1001–1200
2	Normal operation	1201–1350
2	CW valve sticking	1351–1800

codes are available on Ricker's Website.[45] The sampling time is 0.05 h and the set of variables used in the following analysis are given in Table 4.

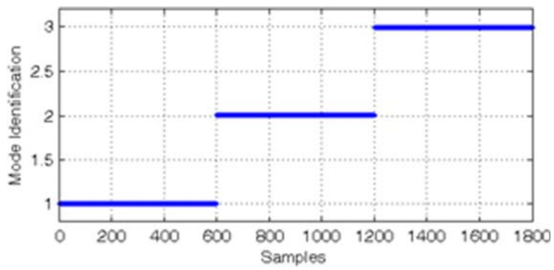

Figure 7. Mode identification result for the test scenario.

[Color figure can be viewed in the online issue, which is available at wileyonlinelibrary.com.]

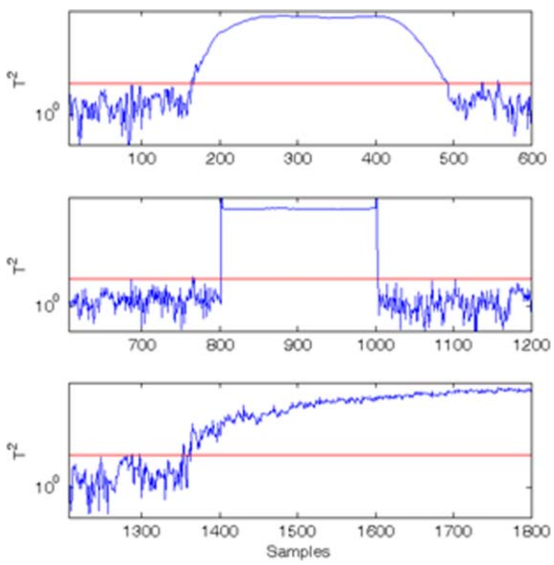

Figure 8. T^2 statistic with 99% control limit (red solid line) for the monitoring of the CSTH process under Mode 3 (top), Mode 1 (middle), and Mode 2 (bottom).

[Color figure can be viewed in the online issue, which is available at wileyonlinelibrary.com.]

Table 4. Variables of the TE Process

Type	Tag	Variable Name	Units
Inputs	u_1	D feed flow rate	kgh^{-1}
	u_2	E feed flow rate	kgh^{-1}
	u_3	A feed flow rate	kscmh
	u_4	A and C feed flow rate	kscmh
	u_5	Purge valve position	%
	u_6	Separator pot liquid flow rate	m^{3}h^{-1}
	u_7	Stripper liquid product flow rate	m^{3}h^{-1}
	u_8	Reactor cooling water flow rate	m^{3}h^{-1}
	u_9	Condenser cooling water flow rate	rpm
Outputs	y_1	A feed	kscmh
	y_2	D feed	kgh^{-1}
	y_3	E feed	kgh^{-1}
	y_4	A and C feed	kscmh
	y_5	Recycle flow rate	kscmh
	y_6	Reactor feed rate	kscmh
	y_7	Reactor temperature	°C
	y_8	Purge rate	kscmh
	y_9	Separator temperature	°C
	y_{10}	Separator pressure	kPAgauage
	y_{11}	Separator underflow	m^{3}h^{-1}
	y_{12}	Stripper pressure	kPAgauage
	y_{13}	Stripper temperature	°C
	y_{14}	Reactor cooling water outlet temperature	°C
	y_{15}	Separator cooling water outlet temperature	°C

Table 5. Test Scenario of the TE Process

Mode	Operating Condition	Period
3	Normal	0–10 h
3	IDV(5): Condenser cooling water inlet temperature	10–20 h
3	Normal	20–30 h
4	Normal	30–45 h
4	IDV(10): C feed temperature	45–55 h
4	Normal	55–65 h
2	Normal	65–72.5 h
2	IDV(4): Reactor cooling water inlet temperature	72.5–80 h
2	Normal	80–90 h
1	Normal	90–105 h
1	IDV(7): C header pressure loss-reduced availability	105–125 h

The TE process is a good example to demonstrate the fault detection capabilities of the proposed combined methodology due to its complexity. To implement the proposed FDI scheme, a set covering 200 h of recorded inputs and

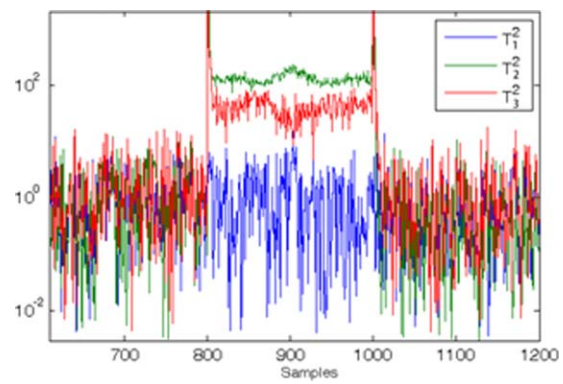

Figure 9. Fault isolation results with tank level sensor (blue line), temperature sensor (red line), and CW flow sensor (green line) decoupled, respectively.

[Color figure can be viewed in the online issue, which is available at wileyonlinelibrary.com.]

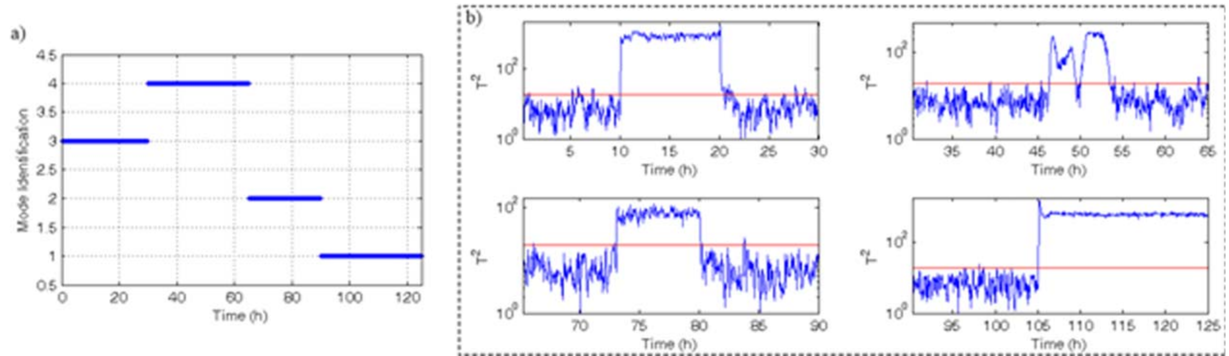

Figure 10. (a) Mode identification result; (b) T^2 statistic with 99% control limit (red solid line) for the monitoring of the TE process under Mode 3 (top left), Mode 4 (top right), Mode 2 (bottom left), and Mode 1 (bottom right).

[Color figure can be viewed in the online issue, which is available at wileyonlinelibrary.com.]

outputs (4000 samples), in which process conditions are switched between the first four operating modes with equal possibilities, is used for offline modeling. By feeding the data into the GMM learning framework, a four-component GMM is obtained. The SMI method is used to generate a linear state-space model with the inclusion of nine state variables for each mode. After the identification of state-space models, a Luenberger observer is constructed for each mode to estimate the state sequence. The T^2 statistic is established on the residual given in Eqs. 5 and 6, followed by the calculation of the control limit with a confidence level of 99%.

To illustrate the fault detection capability of the proposed method, a test scenario given in Table 5 is considered. The total simulation time is 125 h with sampling interval of 3 min. Within this time period, four different operating modes are activated according to the sequence: $3 \rightarrow 4 \rightarrow 2 \rightarrow 1$, and a fault is introduced for some time period during each operating mode. According to the online monitoring procedures developed earlier, the corresponding results are summarized in Figure 10. The left plot in Figure 10a clearly shows that the online mode identification is successful and correct even if some measured samples do not belong to the normal conditions. This is possible because the data sampled under abnormal conditions still achieves maximum posterior probability associated with the corresponding operating modes.

For the purpose of fault detection, the residual generated from the designed UIO for the active operating mode is used to construct T^2 statistic. As illustrated in Figure 10b, the proposed monitoring scheme detects these faults consecutively once an abnormal event occurs in each mode. By comparing the results of Figure 10b with the data in Table 5, it can be observed that each fault is detected almost immediately after it occurs, that the fault detection threshold remains breached for the entire duration of the fault scenario, and that the residual falls below the threshold limit once normal operating conditions are restored.

Finally, it is important to note that in light of the complexity of the TE process (with more than 50 differential equations), the assumption of linear time-invariant state-space representation presents its usefulness and feasibility when a mathematical model is unavailable, and the performance of the combined methodology applied to a large-scale hybrid system like the TE process is also demonstrated.

Conclusions

In this work, a combined data-driven and observer-design methodology was proposed to address the problems of FDI in hybrid process systems. The advantages of the proposed scheme were demonstrated using a numerical simulation example. The proposed method was also applied to recorded data from a simulated CSTH and the well-known TE benchmark process, where the state-space models were identified using SMI. The application studies demonstrated that the combination of data-driven and observer-design techniques has the potential to overcome their respective individual limitations in terms of handling fault isolation in the constituent modes more effectively than is possible with purely data-based methods and, at the same time, avoiding any structural restrictions on the hybrid system required by purely model-based methods for mode identification.

A number of important issues remain to be addressed and are the subject of future research work. For example, the accuracy of the identified state-space models, which depends on the availability and quality of the reference dataset, directly influences the performance of residual generation based on observer-design. Furthermore, the fault distribution matrix is difficult to obtain for industrial applications such that actuator and process fault isolation is still a challenging task. These issues need to be investigated further. The combined methodology, however, offers a promising solution for hybrid process monitoring, which overcomes some of the limitations of both model-based and data-based methods.

Acknowledgments

Financial support from 973 Project of China (2013CB733600), National Natural Science Foundation of China (21176073), Program for New Century Excellent Talents in University (NCET-09-0346), the China Scholarship Council (CSC), and the University of California, Davis are gratefully acknowledged.

Literature Cited

1. Qin SJ. Statistical process monitoring: basics and beyond. *J Chemom.* 2003;17:480–502.
2. Veenkatasubramanian V, Rengaswamy R, Yin K, Kavuri SN. A review of process fault detection and diagnosis: part I: quantitative model-based methods. *Comput Chem Eng*. 2003;27:293–311.

3. Simani S, Fantuzzi C, Patton RJ. *Model-Based Fault Diagnosis in Dynamic Systems Using Identification Techniques*. London: Spring, 2003.
4. Xie L, Kruger U, Lieftucht D, Littler T, Chen Q, Wang SQ. Statistical monitoring of dynamic multivariate process part 1: modeling autocorrelation and cross-correlation. *Ind Eng Chem Res.* 2006;45: 1659–1676.
5. Yoon S, MacGregor JF. Statistical and causal model-based approaches to fault detection and isolation. *AIChE J*. 2000;46:1813–1824.
6. Kruger U, Xie L. *Statistical Monitoring of Complex Multivariate Processes*. Chichester: Wiley, 2012.
7. MacGregor JF, Yu H, Nunoz SG, Flores-Cerrillo J. Data-based latent variable methods for process analysis, monitoring and control. *Comput Chem Eng*. 2005;29:1217–1223.
8. Ding SX. *Model-Based Fault Diagnosis Techniques: Design Schemes, Algorithms, and Tools*. Berlin: Springer, 2008.
9. Patton RJ, Chen J. Observer-based fault detection and isolation: robustness and applications. *Control Eng Pract*. 1997;5:671–682.
10. Sotomayor OAZ, Odloak D. Observer-based fault diagnosis in chemical plants. *Chem Eng J*. 2005;112:93–108.
11. Chang S, You W, Hsu P. Design of general structured observers for linear systems with unknown inputs. *J Franklin Inst*. 1997;334:213–232.
12. Chen W, Saif M. Fault detection and isolation based on novel unknown input observer design. In: Proceedings of the American Control Conference, Minneapolis, Minnesota, 2006.
13. Xiong Y, Saif M. Unknown disturbance inputs estimation based on a state functional observer design. *Automatica*. 2003;39:1389–1398.
14. Gao Z, Ding SX. Sensor fault reconstruction and sensor compensation for a class of nonlinear state-space systems via a descriptor system approach. *IET Control Theory Appl*. 2007;1:578–585.
15. Schubert U, Kruger U, Arellano-Garcia H, Feital TDS, Wozny G. Unified model-based fault diagnosis for three industrial application studies. *Control Eng Pract*. 2011;19:479–490.
16. Chiang L, Russell E, Braatz R. *Fault Detection and Diagnosis in Industrial Systems*. London, Great Britain: Springer-Verlag, 2001.
17. Favoreel W, Moor BD, Overschee PV. Subspace state space system identification for industrial processes. *J Process Control*. 2000;10: 149–155.
18. Yu J, Qin SJ. Multimode process monitoring with Bayesian inference-based finite Gaussian mixture models. *AIChE J*. 2008;54: 1811–1829.
19. Qin SJ. Survey on data-driven industrial process monitoring and diagnosis. *Annu Rev Control*. 2012;36:220–234.
20. Ding SX, Zhang P, Naik A, Ding EL, Huang B. Subspace method aided data-driven design of fault detection and isolation systems. *J Process Control*. 2009;19:1496–1510.
21. Schubert U, Kruger U, Wozny G, Arellano-Garcia H. Input reconstruction for statistical-based fault detection and isolation. *AIChE J*. 2012;58:1513–1523.
22. Ohran BJ, Peña DM, Davis JF, Christofides PD. Enhancing data-based fault isolation through nonlinear control. *AIChE J*. 2008;54: 223–241.
23. Ohran BJ, Liu J, Peña DM, Christofides PD, Davis JF. Data-based fault detection and isolation using feedback control: output feedback and optimality. *Chem Eng Sci*. 2009;64:2370–2383.
24. Hu Y, El-Farra NH. Robust fault detection and monitoring of hybrid process systems with uncertain mode transitions. *AIChE J*. 2011;57: 2783–2794.
25. Zhao SJ, Zhang J, Xu YM. Monitoring of processes with multiple operating modes through multiple principal component analysis models. *Ind Eng Chem Res*. 2004;43:7025–7035.
26. Feital T, Kruger U. Dutra J. Pinto JC, Lima EL. Modeling and performance monitoring of multivariate multimodal processes. *AIChE J*. 2013;59:1557–1569.
27. Duda RO, Hart PE, Stork DG. *Pattern Classification*, 2nd ed. New York: Wiley, 2001.
28. Figueiredo MAF, Jain AK. Unsupervised learning of finite mixture models. *IEEE Trans Pattern Anal Mach Intell*. 2002;24:381–396.
29. Hu W, Choi KS, Gu Y, Wang S. Minimum-maximum local structure information for feature selection. *Pattern Recognit Lett*. 2013;34: 527–535.
30. Jiménez-Rodríguez LO, Arzuaga-Cruz E, Vélez-Reyes M. Unsupervised linear feature-extraction methods and their effects in the classification of high-dimensional data. *IEEE Trans Geosci Remote Sens*. 2007;45:469–483.
31. Cai D, He X, Han J. Document clustering using locality preserving indexing. *IEEE Trans Knowl Data Eng*. 2005;17:1624–1637.
32. Qin SJ. An overview of subspace identification. *Comput Chem Eng*. 2006;30:1502–1513.
33. Overschee PV. Subspace identification for linear systems, 2002. Available at: http://www.mathworks.com/matlabcentral/. Accessed on April 2013.
34. Saif M, Guan Y. A new approach to robust fault detection and identification, *IEEE Trans Aerosp Electron Syst*. 1993;29:685–695.
35. El-Farra NH, Ghantasala S. Actuator fault isolation and reconfiguration in transport-reaction processes. *AIChE J*. 2007;53:1518–1537.
36. Ghantasala S, El-Farra NH. Robust actuator fault isolation and management in constrained uncertain parabolic PDE systems. *Automatica*. 2009;45:2386–2373.
37. Giridhar A, El-Farra NH. A unified framework for detection, isolation and compensation of actuator faults in uncertain particulate processes. *Chem Eng Sci*. 2009;64:2963–2977.
38. Kourti T. Multivariate dynamic data modeling for analysis and statistical process control of batch processes, start-ups and grade transitions. *J Chemom*. 2003;17:93–109.
39. Zhu Z, Song Z, Palazoglu A. Transition process modeling and monitoring based on dynamic ensemble clustering and multiclass support vector data description. *Ind Eng Chem Res*. 2011;50:13969–13983.
40. Thornhill NF, Patwardhan SC, Shah SL. A continuous stirred tank heater simulation model with applications. *J Process Control*. 2008; 18:347–360.
41. Thornhill NF, Patwardhan SC, Shah SL. The CSTH simulation, 2007. Available at: http://personal-pages.ps.ic.ac.uk/~nina/CSTHSimulation/index.htm. Accessed on April, 2013.
42. Downs JJ, Vogel EF. A plant-wide industrial process control problem. *Comput Chem Eng*. 1993;17:245–255.
43. Zhu ZB, Song ZH, Palazoglu A. Process pattern construction and multi-mode monitoring. *J Process Control*. 2012;22:247–262.
44. Ricker NL. Decentralized control of Tennessee Eastman challenge process. *J Process Control*. 1996;6:205–221.
45. Ricker NL. Tennessee Eastman challenge archive, 2002. Available at: http://depts.washington.edu/control/LARRY/TE/download.html. Accessed on Sept. 2012.

Manuscript received Jan. 23, 2014, and revision received Apr. 8, 2014.